

HULL SHAPE DESIGN OF A COMPRESSED NATURAL GAS SHIP

E.B. Malta, M.C. Nogueira, A.A. Ramos, C.M. Sampaio

TPN-Numerical Offshore Tank

University of São Paulo, Brazil

ABSTRACT In order to design the hull shape of a compressed natural gas ship (CNG), a parametric model was integrated with forward resistance and seakeeping commercial codes. This integration allowed dynamic results analysis using only a program interface with external codes experimentally verified. With regard to motions in waves, potential and strip method were used to evaluate the RAO (Response Amplitude Operator) of the hull forms in different conditions (with / without forward speed). The seakeeping has been defined through acceleration and comfort indices based on spectral analysis. The forward resistance was determined using non-linear potential method for the wave resistance and finite volume method without free surface effect for the viscous resistance. Both numerical models were validated with results achieved in the IPT towing tank. The evaluation of some design output parameters, generated with the parametric model, assist to determine which variables influence the most in CNG ship forward resistance and seakeeping. The same methodology can be applied in other type of hull shape designs.

1 INTRODUCTION

The lack of pipelines to transport natural gas required the development of alternatives which can efficiently transfer the production to the coast. One solution is to use vessels capable of transporting the compressed natural gas (CNG). In these ships design, hull lines are set to efficiently carry a certain amount of gas, reducing fuel consumption by reducing the forward resistance and maintaining acceptable levels of motion in waves.

Nowadays, numerical simulators are an important tool to design any offshore systems due to its capacity of evaluating a large number of conditions in a virtual environment, which would have higher costs and take a lot of time to do in towing tanks. For that reason, it was created a parametric model at *Friendship Framework* [1] together with other commercial codes that were first verified with some preliminary experiments. The main dimensions used to build the model were lengths, beams and heights as will be explained better at "Design Methodology" chapter. Besides these main dimensions, other parameters were used to change different aspects of the hull shape, varying slopes, angles and parameters related to stern and bulbous bow[2].

For the analysis of many hull shapes, it was created integration between the parametric model and some analysis programs for resistance forces and seakeeping. In order to evaluate the resistance force, it was used *Shipflow* program [3] for the wave generation resistance using XPAN subroutine based on potential method. For the viscous resistance, it was used Star-CCM +[®], which performs the calculations using the finite volume method.

With regard to the motion in waves, *Seakeeper* [4], which is based on the strip method in the frequency domain, was used to obtain the RAO's (*Response Amplitude Operator*). The results reliability was assured with experimental results comparison. Another possibility was to evaluate ship motions using potential method with *Rankine* sources distribution along the hull and free surface. Nevertheless, this assessment requires more computational time which makes it difficult to implement in the optimization process. Therefore, the RAO results of *Seakeeper* defined acceleration and comfort indices based on spectral analysis [5].

After defining the most relevant parameters for each analysis and the intervals at which the model is valid, some evaluation methods were applied to define the parameters that most influence the design.

2 DESIGN METHODOLOGY

Vessel design process involves a series of tests among which there are: stability, forward resistance, seakeeping, maneuverability, hull-propeller-engine performance and structural analysis.

The need for these analyses during the design process motivates integrated models. Among the analyses that can be integrated, the focus of this work was the integration of the forward resistance and seakeeping evaluations. In summary, the methodology is initiated using the routines that help to determine the main dimensions using the information available in references as [6] and [7]. These dimensions are entries to the parametric hull model where the analyses can be performed and the results verified according to pre-established requirements. Thus the methodology for the vessel design is summarized in Figure 1.

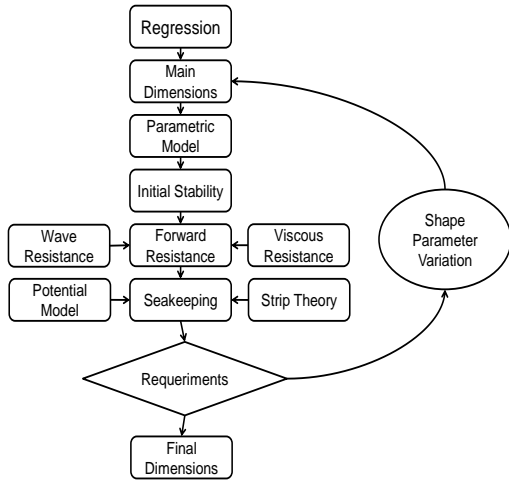


Figure 1: Design Methodology

First, the initial main dimensions were obtained by the regressions in [6] and [7], which are described in Matlab routines [8]. For instance, these routines are used to define the necessary displacement based on transport capacity and other design requirements, so the initial main dimensions can be set to construct the hull surface.

With this parameterization and all model evaluations described above, it was possible to define a CNG ship hull. The same methodology can be applied to other vessels designs.

3 PARAMETER DESCRIPTION

For the hull surface construction, it was necessary to establish some design parameters from the dimensionless variables input. These parameters and dimensionless variables are listed below, with a brief description of their roles in the project.

3.1 INPUT PARAMETERS

The hull was divided into three areas: bow, stern and parallel body. It was created two parameters to define their length: the bow length (L_{bow}) and the parallel body length (L_{body}). The stern length is defined as the total length minus bow and parallel body lengths.

Throughout the hull, points were placed to form the body plan. These points were interpolated by ten *spline* curves, named as B00 up to B09, which were used to construct the surfaces as presented at Figure 2.

To set the angle with which the ship cuts the water, there is a parameter called ($bow_angle | L_{bow}$), which provides the relationship as the section B07 is positioned in proportion to the length of the bow defined by the section B06.

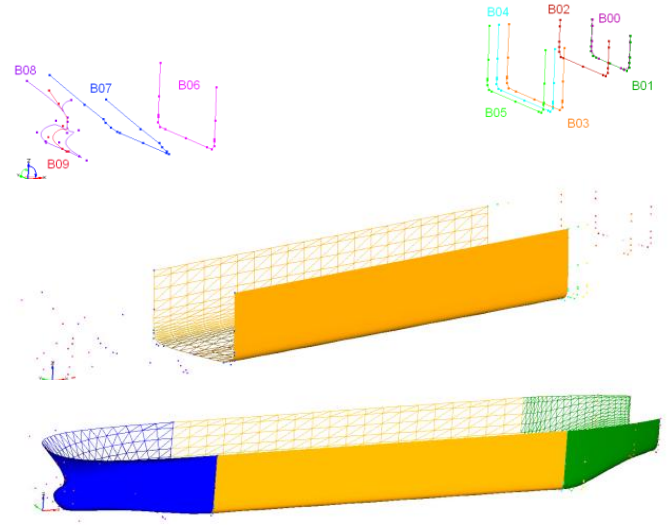


Figure 2: Hull surface creation

3.2 Bow parameters

Bow parameters are bow length, rake, stem and flare. The *rake* is the length in the x-axis where the deck is forward of the stem. The *stem* is defined in the z-axis direction, which provides the beginning of the *rake* above the water. The dimensionless distance of the *flare* is the distance in the deck at the y-axis, as presented in Figure 3.

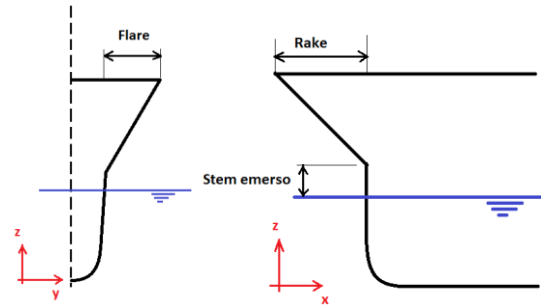


Figure 3: Rake, flare and stem parameters

3.3 Bulb parameters

The bulb is defined from sections B08 and B09 set of points. The first point that was parameterized sets the height (H_b), in which the bulb starts from the hull stem.

The remaining points are positioned in pairs, one point in the section B09, with their coordinates in a XZ plane and the other in section B08 with the same coordinates in XY plane. The points are divided to set its z coordinate as ZBA, ZBB and BMZ. The parameters to set y coordinates on the section B08 are BBA, BBM and BBB, as shown in Figure 4. The bulb length is obtained with the parameters L_{prAB} , positioning in the x-axis direction, along with the midpoints L_{prm} .

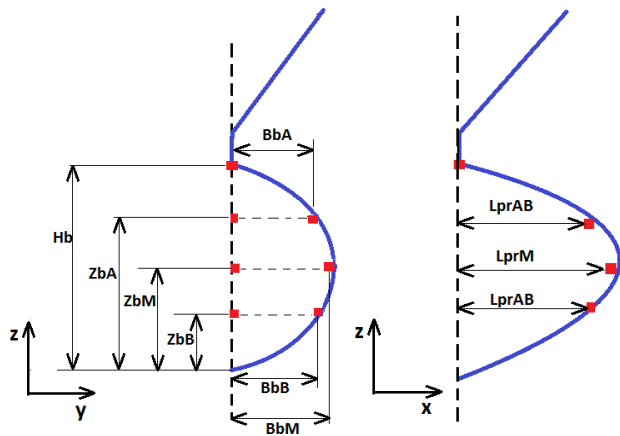


Figure 4: Bulb variables

3.4 Stern parameters

Input parameters that define the stern are *transom* stern beam (Btransom / Boca), stern *transom* immersion (immersion of the stern / draft), which define aft frame's points (B00 to B02). It was created two frames which positions are responsible for stern slope (B02 and B03). B02 and B03's position were set as parameters called initial stern slope and final stern slope.

Stern tangent refers to B00, B01 and B03 stern slope in the y direction.

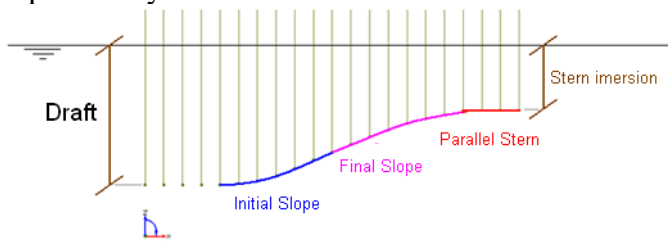


Figure 5: Input parameters of the stern - side view



Figure 6: Input parameters of the stern - top view

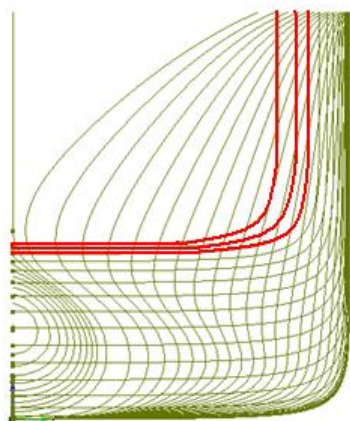


Figure 7: Input parameters of the stern - front view

3.5 HYDROSTATIC EVALUATION

The hydrostatic parameters are obtained through the curve of the sectional area shown in Figure 8. These parameters are: the *center of buoyancy*, which is the center of the submerged volume; the *center of floatation* which is located the center in the water line area; the *line area* and *longitudinal and transverse moments* both in the area of water line.

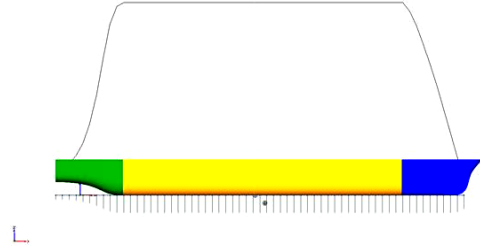


Figure 8: Sectional area curve.

3.6 MOTION IN WAVE EVALUATION

The performance evaluation of a ship in waves is essential, both to ensure the integrity of the vessel as to ensure the conditions of comfort and safety of crew and cargo.

The model of wave behavior was analyzed by integrating with the programs that uses method of panels and strip theory for effecting their calculations.

The *Seakeeper* program is based on the strip theory in the frequency domain. The main advantage is the reduced computational time to obtain the hydrodynamic properties of two-dimensional sections through the hull, which after integration along the length of the vessel, resulting in coefficients of added mass, damping and excitation forces in waves. With these hydrodynamic coefficients can be obtained from the movements of the vessel and, consequently, the *RAO*.

In the case of the method of panels, it uses *Ran-kine* sources in the time domain, the distribution of tiles along the hull and free-surface to thereby solve the potential flow associated, resulting in greater accuracy at the cost greater computational effort.

From the results of both methods was performed a comparison between the numeric *RAO*'s and the experimental tests performed in the Instituto de Pesquisas Tecnológicas (IPT), as shown in Figure 9 and Figure 10.

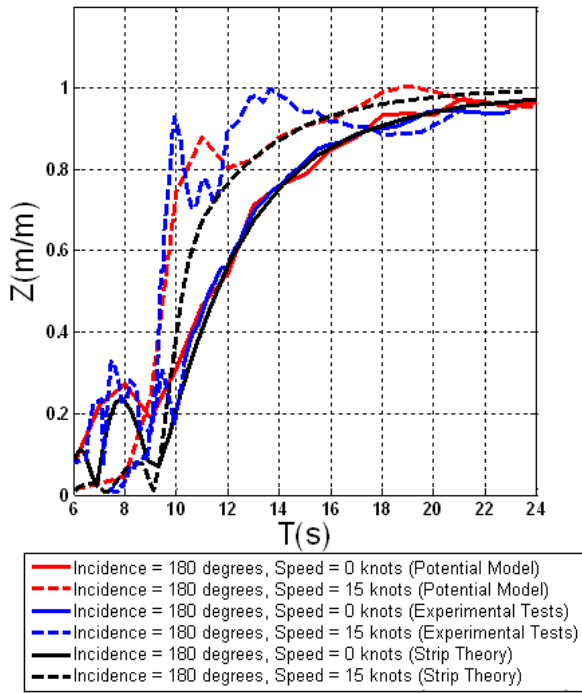


Figure 9: Comparison of *Heave* RAO

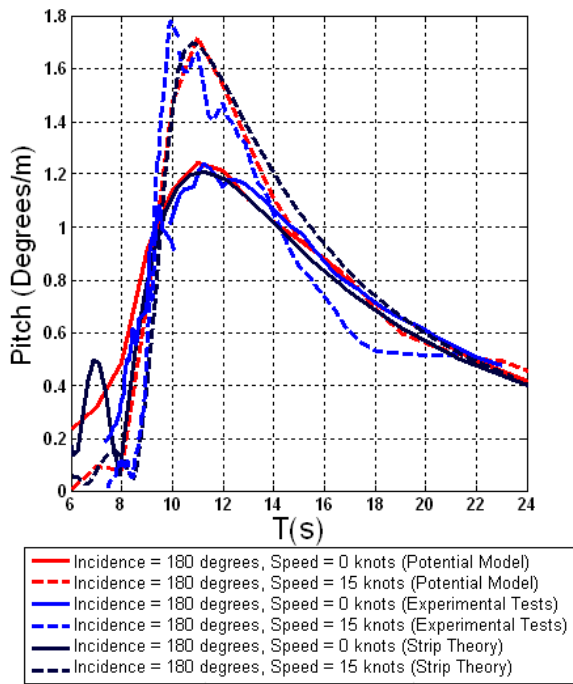


Figure 10: Comparison of *Pitch* RAO

Thus, it is observed that although the method panels presents a better grip with the tests, the strip theory (*Seakeeper*) shows a good trend and it is more appropriately to be use in the process of optimizing behavior in waves.

From the results obtained in *Seakeeper* is possible through spectral crossover between the *RAO* of the vessel and a *JONSWAP* sea spectrum, obtaining the performance against two criteria of comfort: *Motion Sickness Incidence* (MSI) [6] and *Subjective Motion* (SM) [5].

3.7 WAVE RESISTANCE EVALUATION

The subroutine *XPAN* is the module responsible for calculating the potential flow. As the output parameter coefficient of hull wave profile is obtained by waves generated by the hull as shown in Figure 11.

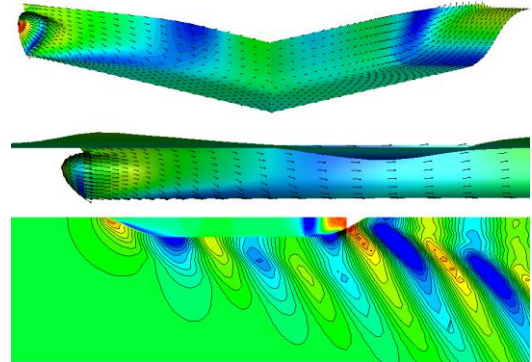


Figure 11: Visualization of flow around the hull through *XPAN*

For the hull was made an initial comparison of numerical results with the experimental results, the coefficient of wave from the experimental test was obtained from C_T (total coefficient of resistance) across regressions (see ref [6]).

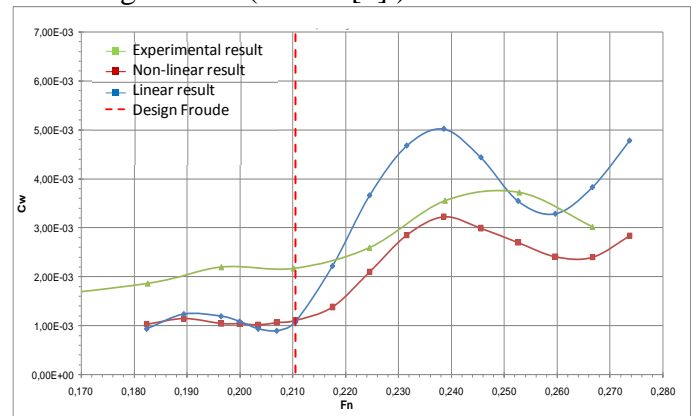


Figure 12: Wave resistance comparison

3.8 VISCOUS RESISTANCE EVALUATION

In order to obtain the viscous resistance component, hull submerged parts were modeled in *Star-CCM+*[®], which performs calculations with finite volume method.

The phenomenon of interest occurs in steady state, which lead to the use of *RANS* (*Reynolds Averaged Navier-Stokes Equation*) as a simplification of Navier-Stokes equations. To complete *RANSE*, standard $k-\epsilon$ turbulence model was chosen. Boundary layer was modeled using wall function.

The computational domain dimensions, important for the use of correct boundary conditions, were defined based on [11] and [12].

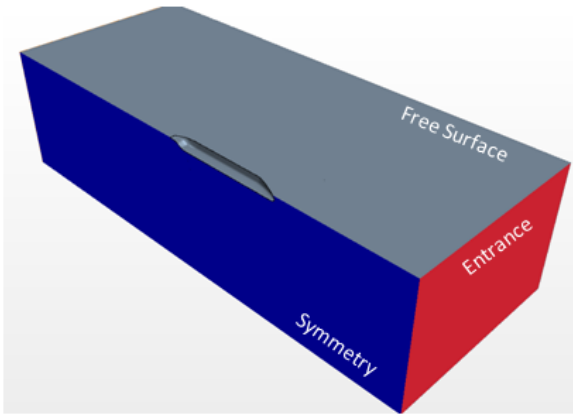


Figure 13: Computational domain

Table 1: Dimensions of the computational domain

Direction	Size (* Lbp)
Forward	1
Aft	2
Depth	1.5
width	1

The boundary conditions that were applied, shown in the table below, are widely used and can be found in several publications.

Table 2: Boundary conditions

Surface	Boundary Condition	Mathematical Expression
Ship	Full adherence	$V = 0$
Entrance Plan	evanescence	$V = V_{away}$
Exit Plan		$p = p_{atm}$
Symmetry Plan	Symmetry	-
Free Surface	Impermeability	$v \cdot n = 0$
Lateral wall		
Bottom Plan		

Hexahedron mesh was used, which is recommended scenario for external flow and which generation time is much lower than polyhedral mesh. The grid was block-structured, i.e., the domain is divided into sub-regions in which the element size is determined by the user. The advantage is the ability to refine only regions necessary for capturing the physical phenomena investigated, avoiding the generation of unnecessary elements and reducing the mesh size. The domain was divided into four sub-regions (Figure 14 and Figure 15).



Figure 14: Block-structured mesh hexahedral (side view)



Figure 15: Block-structured mesh hexahedral (side view)

In two sub-regions, the elements are larger in the x direction, since this is the predominant flow direction, with more intense velocity gradients that do not require a mesh as fine as in the other directions to be captured.

A prism layer mesh was also generated in which a wall function was used to model boundary layer (Figure 16).

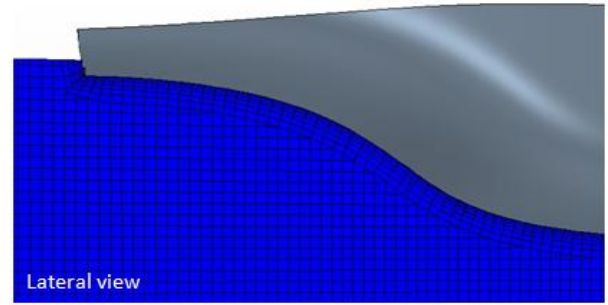


Figure 16: Prismatic mesh detail at the stern of the vessel (side view)

The mesh has approximately 500,000 elements, being considered light.

This model was compared with experimental test performed at the IPT. For Froude numbers between 0.07 and 0.21, the difference between numerical and experimental results was less than 4%.

4 MODEL RESULTS

The seakeeping and resistance analysis are presented in this chapter.

4.1 SEAKEEPING RESULTS

The seakeeping analysis made possible to get an insight of the relation between parameters variation and comfort levels at the deck (SM and MSI). The condition considered was head seas at speed of 15 knots with 3.5m of significant height and 9s of peak period spectrum.

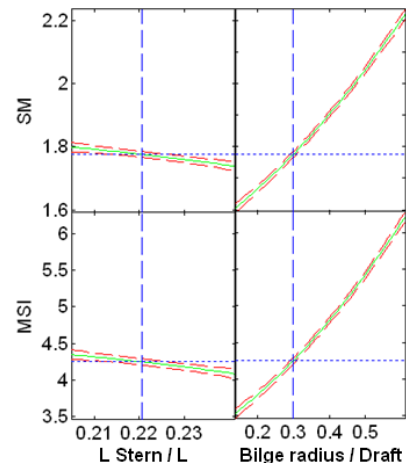


Figure 17: Influences on MSI and SM

The parameter which influences SM and MSI the most is the non-dimensional bilge radius (Figure 17), causing 40% and 26% variation in MSI and SM,

respectively. Its reduction from 0.3 to 0.15 improves about 16% and 9% of the initial hull MSI and SM.

Bow angle, parallel body length, and bow length had minor influence in comfort level. The variation of the three parameters together results in 12% and 7% change in MSI and SM, respectively. Their increase until the maximum range value improved 7.5% and 4% of the initial hull MSI and SM.

The section B07 inclination had similar results but the comfort levels were increased. Non-dimensional bow radius had practically no influence over sea-keeping. A summary of this analysis is showed in Table 3.

Table 3: Trend of the hull parameters according to comfort index

↑	MSI and SM tendency
Bow angle	↘
Parallel Length	↘
Bow Length	↘
Bilge radius	↑
B07 inclination	↗
Bow radius	-

Figure 18 show MSI and SM, respectively, according to bilge radius and bow length, the two parameters which influenced the most in sea-keeping.

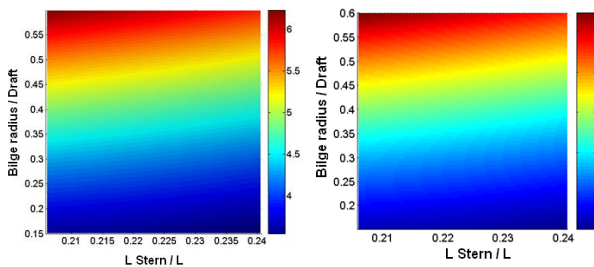


Figure 18: Bilge radius and stern length influence on MSI and SM

4.2 WAVE RESISTANCE RESULTS

4.2.1 Linear analysis of the hull

Through an analysis of all parameters of the bulb was observed that the parameters associated with longitudinal format (as shown in Figure 19) have influence a lot like each other. The same effect can be noticed in other directions, thus, were chosen for the study, the average parameters for each direction.

In Figure 19 it is evident the growing influence of the width of the bulb and descending of the parameters that define width and height.

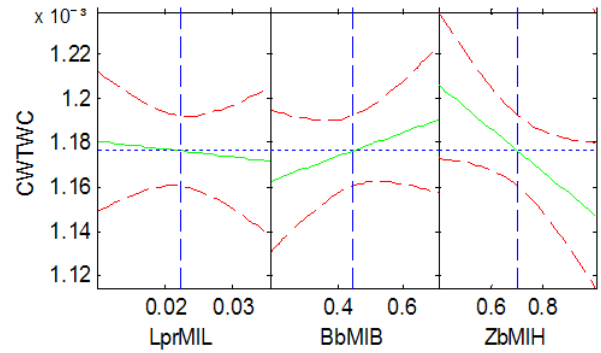


Figure 19: Influence in CWTWC for the linear

Changing ZbM from 0.7 (initial value) to 1 reduces the wave coefficient about 2.3%, while the change of the other two parameters together cause a reduction of 1.5%.

The parameters combined influence can be seen in Figure 20 and Figure 21.

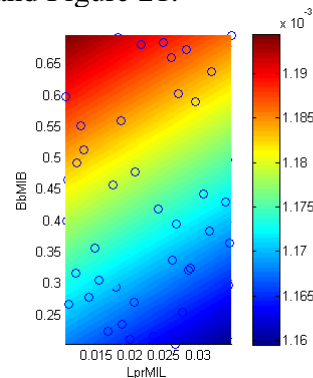


Figure 20: Variation of CWTWC depending on the width and length of the midpoints of the bulb

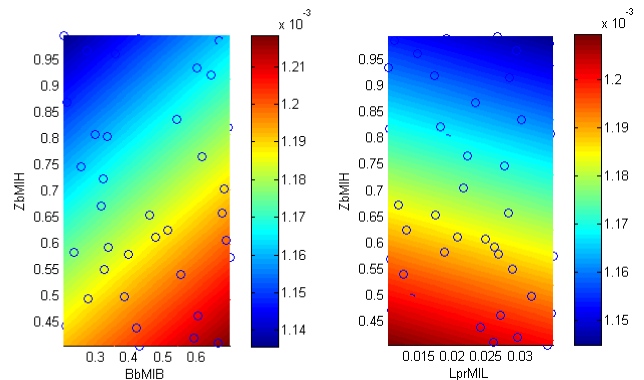


Figure 21: Variation of CWTWC depending on the width and height of the midpoints of the bulb

Wave making resistance had a 8.4% reduction compared to the original hull. 500 hulls, generated using Sobol, were evaluated. Figure 22 shows pressure distribution on the mean draft of the original hull (top) and the one with smaller wave resistance (bottom). Figure 23 shows the comparison between the hull's frames

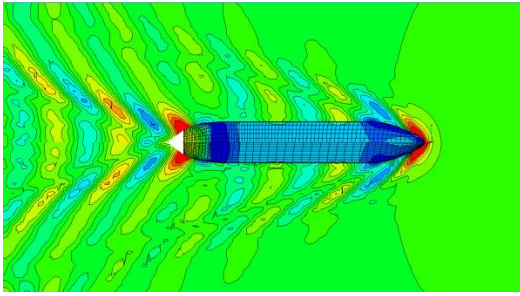


Figure 22: Linear wave generation of bow optimization (Original at top and least wave resistance at bottom)

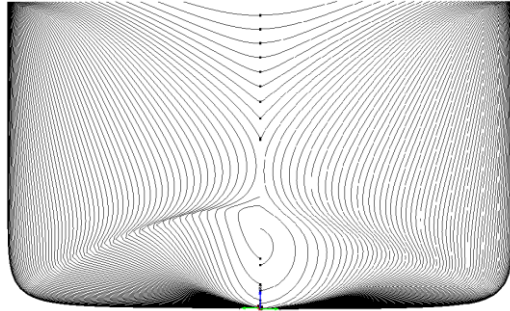


Figure 23: Body plan comparison with linear free surface (Original at right and least resistance at left)

4.2.2 Nonlinear resistance of the hull

In order to obtain more accurate results and to verify if the linear theory provides sufficient results, a non-linear analysis was made. Due to higher time consumption, fewer hulls were investigated.

As in the analysis of linear free-surface, the parameters for the same direction showed a similar influence on CWTWC.

In Figure 24, the influences of medium parameters in CWTWC bulb, with its parameters of length, width and height behaved very similar conditions with linear free-surface.

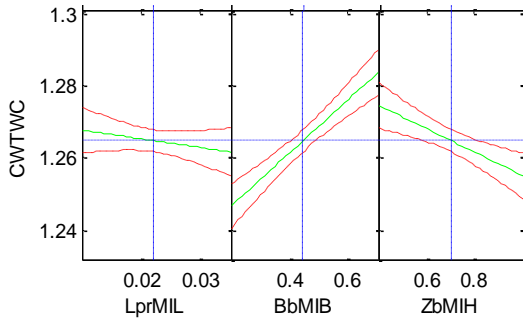


Figure 24: Influences on CWTWC for free-surface nonlinear hull

The parameter BBM showed a greater influence and provided an improvement of approximately 1.4%. In the case of the BMZ, which had been the most influential in the linear case, the improvement was only 0.7%. The parameters combined influence can be seen in Figure 25 and Figure 26.

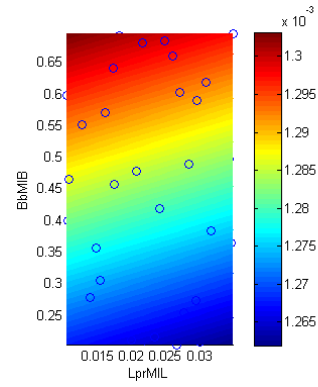


Figure 25: Variation of CWTWC depending on the width and length of the midpoints of the bulb

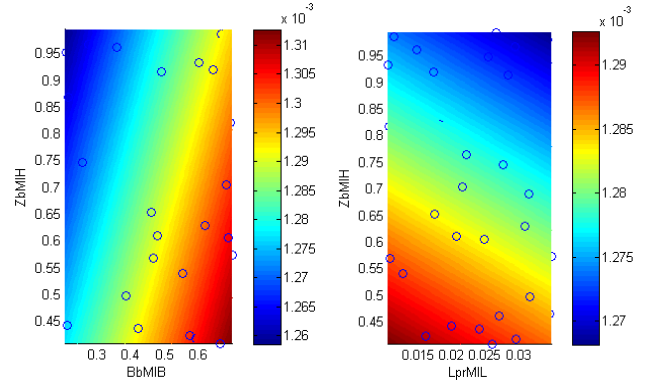


Figure 26: Variation of CWTWC depending on the width and height of the midpoints of the bulb

Figure 24 shows pressure distribution on the mean draft of the original hull (top) and the one with smaller wave resistance (bottom). Figure 25 shows the comparison between the lowest wave resistance hulls's frames and the original one.

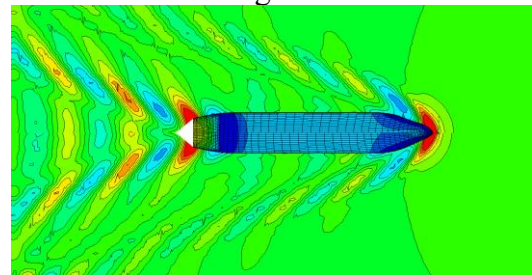


Figure 27: Non-linear waves generation of bow optimization (Original at top and least wave resistance at bottom)

The hull with lowest wave resistance obtained through linear and non-linear methods have similar frames.

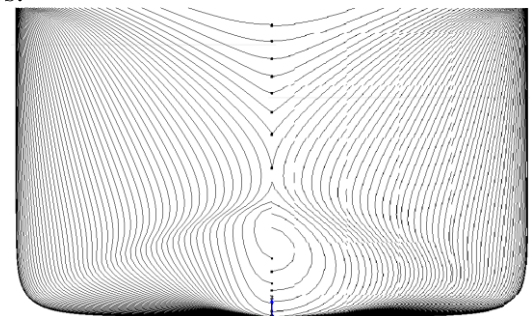


Figure 28: Body plan comparison with non-linear free surface (original at right and hull with least resistance at left)

4.2.3 Stern shape influence in non-linear wave resistance

The stern parameters investigated to evaluate wave generation resistance were:

- Stern initial slope;
- Parallel Stern;
- Stern tangent;
- Stern immersion/Draft;
- Transom beam/Total Beam;
- Stern final slope.

Initially, a study was conducted to determine which parameters most influence on the wave coefficient. Sobol was used to generate 298 hulls. Wave coefficient variation according to 6 stern parameters can be observed in Figure 29 and Figure 30.

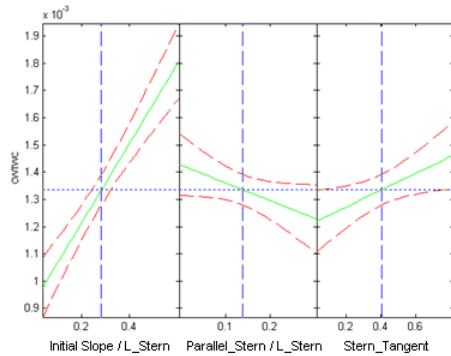


Figure 29: Influence of initial stern slope, parallel stern and stern tangent in CWTWC

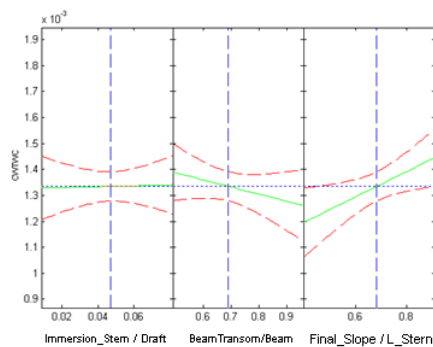


Figure 30: Influence of stern immersion stern, transom beam and final stern slope in CWTWC

Stern initial slope, stern final slope and stern tangent are the parameters that most influenced wave making resistance. They were set as variables in an optimization process using the tangent method and a 28.8% wave resistance reduction (relative to original hull) was achieved.

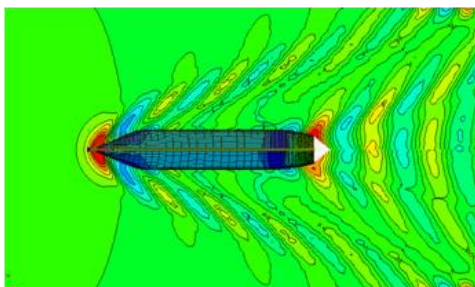


Figure 31: Non-linear waves generation of stern optimization (Original at top and least wave resistance at bottom)

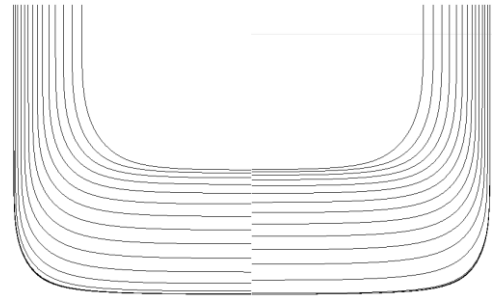


Figure 32: Comparison of the stern body plan (Original at right and least wave resistance at left)

4.2.4 Stern shape influence in viscous resistance

The viscous resistance results of the 243 hulls generated with the variation of stern parameters (final slope, initial slope, transom beam, immersion and stern tangent) were organized in such a manner that one can note which parameters influence the most. Small changes of block coefficient, longitudinal center of buoyancy position, wetted surface and displacement were made (up to 2%).

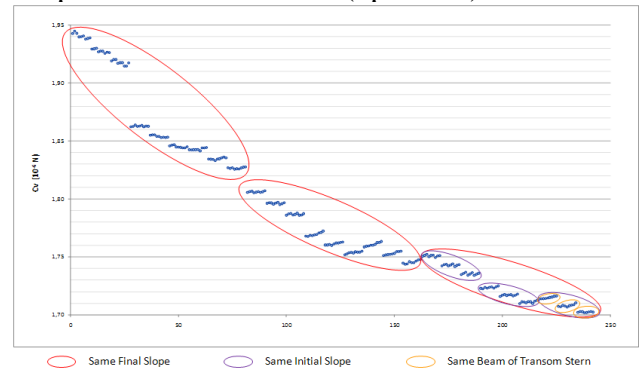


Figure 33: Viscous resistance evaluation of stern parameters

In Figure 33, points inside same red ellipse have same final slope, the ones contained in a purple ellipse have same initial slope and the ones contained in a yellow ellipse have same transom breadth.

Also in Figure 33 evidences that final and initial slope, respectively, are the parameters which influence viscous resistance the most.

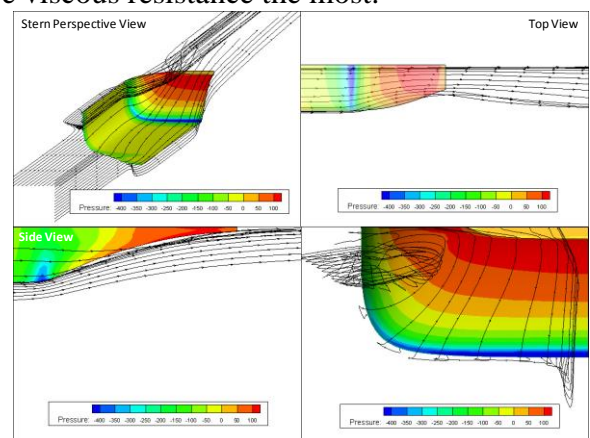


Figure 34: Pressure distribution and streamlines (wave resistance optimum hull)

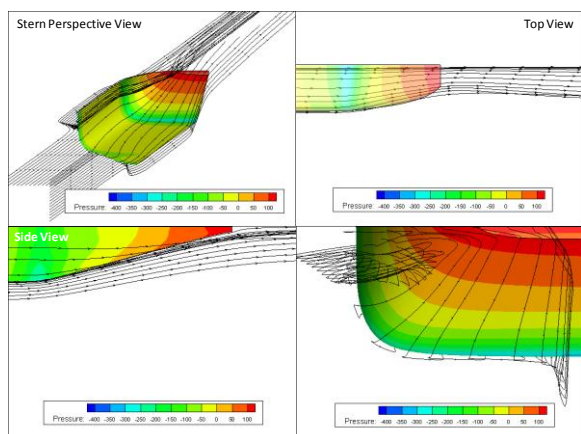


Figure 35: Pressure distribution and streamlines (least viscous resistance hull)

Viscous resistance reduction is observed along with vortex size reduction and aft pressure increase. Figure 34 and Figure 35 show stern pressure distribution and flow streamlines of the wave resistance optimum hull and the least viscous resistance hull, respectively. Their geometry differences can be seen in the side view. In the back and perspective views of Figure 34, an intense vortex can be observed at the vessel's shoulder. The vortex decrease in size can be seen in the back and perspective views of Figure 35. With regards to aft pressure, the back view shows higher intensity and homogeneity in the least viscous resistance hull.

5 CONCLUSIONS

The hull shape for natural gas transportation was designed considering seakeeping and ship resistance.

For that it was developed a parametric model in the program FriendShip and it was performed an evaluation of the input and output parameters. This was achieved through the parametric model, where the surfaces were defined by points according to the size of the main vessel.

With this model it was possible to monitor seakeeping trends of each parameter in the comfort indices MSI and SM. By the model based on strip method, comfort levels were more influenced by the bilge radius, where it was possible to improve the original hull at 16% in MSI and 9% in SM.

The ship resistance results have been made by Transverse Wave Cut Method considering the free-surface (linear and nonlinear) and comparisons of the two hulls (with and without bulbous bow). Hull without bulb was evaluated the influence only of the main dimensions with linear free-surface. For the case of bulbous bow, different conditions of free surface, generate different magnitudes of influence. For the linear free-surface the parameter of greatest influence was BMZ, with a reduction of 2.5% in wave making resistance, while for the nonlinear free-surface the parameter BBM decreased the coefficient by 1.4%.

So with this parametric model is possible to optimize the hull with the definition of an objective function in terms of ship resistance and seakeeping. This methodology could be used in other vessel types to design ship considering the most influenced parameters.

6 ACKNOWLEDGEMENTS

The authors would like to thank TRANSPETRO for all the support during this project.

7 REFERENCES

- [1] Abt, C., Bade, SD, Birk, L., Harries, S. Parametric Hull Form Design – A Step Towards One Week Ship Design, 8th International Symposium on Practical Design of Ships and Other Floating Structures PRADS 2001,
- [2] Kracht, AM; "Design of Bulbous Bows", Transactions SNAME, Vol. 86, 1978.
- [3] Flowtech International ab, "SHIPFLOW USER MANUAL", Gotenburgo, SUÉCIA, 2008.
- [4] Seakeeper user manual, Formation Design Systems Pty Ltd 1998 – 2009.
- [5] Lloyd, ARJM; "Seakeeping: Ship Behaviour in Rough Weather", Chapter 21 – Effects of ship motions on passengers and crew; Ellis Horwood Limited; 1989.
- [6] Watson, D, G.; "Practical Ship Design"; Elsevier Ocean Engineering Book Series; 1998
- [7] Lewis, EV (Editor); "Principles of Naval Architecture"; SNAME, 2 nd Edition, New York, SNAME, 1989.
- [8] MATLAB USER MANUAL
- [9] Stromgren, C.; "A comparison of Alternative Bow Configurations"; Marine Technology, vol. 32, 1995. 32, 1995.
- [10] Benford, H. Benford, H. "Naval Architecture for Non-Naval Architects", Jersey City, NJ, 1991, 239p.
- [11] Ahmed Y.; Soares CG Simulation of free surface flow around a VLCC hull using viscous and potential flow methods. Ocean Engineering, Volume 36, pp. 691-696, 2009.
- [12] Choi JE et al., Resistance and propulsion characteristics of various commercial ships based on CFD results. Ocean Engineering, Volume 37, pp. 549–566, 2010.